



RESEARCH ARTICLE

10.1002/2017EF000588

Key Points:

- The N + S deposition lead to 2.92 times more critical load exceeded areas than N deposition in 2000s
- Critical load (CL) exceedance by N deposition is dominated by NO_y in 2000s but likely by NH_x in 2050s
- The projected increase of air temperature can lead to fewer CL exceeded areas in 2050s

Supporting Information:

- Supporting Information S1

Corresponding author:

J. S. Fu, jsfu@utk.edu

Citation:

Sun, J., J. S. Fu, J. A. Lynch, K. Huang, and Y. Gao (2017), Climate-driven exceedance of total (wet + dry) nitrogen (N) + sulfur (S) deposition to forest soil over the conterminous U.S., *Earth's Future*, 5, doi:10.1002/2017EF000588.

Received 31 MAR 2017

Accepted 25 APR 2017

Accepted article online 28 APR 2017

Climate-driven exceedance of total (wet + dry) nitrogen (N) + sulfur (S) deposition to forest soil over the conterminous U.S.

Jian Sun¹, Joshua S. Fu^{1,2}, Jason A. Lynch³, Kan Huang^{1,4}, and Yang Gao⁵

¹Department of Civil and Environmental Engineering, University of Tennessee, Knoxville, Tennessee, USA, ²Climate Change Science Institute and Computational Sciences and Engineering Division, Oak Ridge National Laboratory, Oak Ridge, Tennessee, USA, ³Clean Air Markets Division, U.S. Environmental Protection Agency, Washington, DC, USA,

⁴Center for Atmospheric Chemistry Study, Shanghai Key Laboratory of Atmospheric Particle Pollution and Prevention (LAP3), Department of Environmental Science and Engineering, Fudan University, Shanghai, China, ⁵Key Laboratory of Marine Environment and Ecology, Ministry of Education of China, Ocean University of China, Shandong, China

Abstract Nitrogen (N) and sulfur (S) depositions are much mitigated over the conterminous U.S. (CONUS) but deposition exceedance still exists on forest soil. In addition, the empirical approach is usually used but only provides a spatially constant critical load (CL). Therefore, the CL derived from steady-state mass balance equation is used to study the CL exceedance on forest soil over the CONUS. The multimodel mean (MMM) of global climate-chemistry models in 2000s indicates that total (wet + dry) N deposition alone over 10.32% of forest soil exceeds the CL, but a higher percent (30.16%) is observed by the N + S deposition, which highlights the necessity of considering S deposition. In 2050s, less CL-exceeded forest soil is projected and the exceedance amount is lower as well, mainly attributed to the strong reduction of projected NO_x and SO_2 emissions. By first projecting the future CL due to the climate change, the CL exceedance could further decrease as the air temperature is projected to increase rapidly and lead to higher CL in the future. The CL exceedance by N deposition alone is likely to be dominated by NO_y in 2000s but NH_x in 2050s because of the enhanced NH_3 emission. Moreover, both in 2000s and 2050s, using the CL generated by different aggregation methods can cause up to 33 times difference between the corresponding CL exceedance. This suggests that several regions are under the marginal threat of either N or N + S deposition and different CL can influence the results significantly.

1. Introduction

Human activities including fossil fuel combustion and fertilizer production have contributed significantly to the emission of reactive nitrogen N_r {oxidized nitrogen ($\text{NO}_y = \text{NO} + \text{NO}_2 + \text{NO}_3^- +$ other inorganic [e.g., N_2O_5] and organic components [e.g., PAN]) and reduced nitrogen ($\text{NH}_x = \text{NH}_3 + \text{NH}_4^+$)} and SO_x ($\text{SO}_2 + \text{SO}_4^{2-}$) in the past decades [Olivier *et al.*, 1996; Vitousek *et al.*, 1997; Smith *et al.*, 2001; Galloway *et al.*, 2004]. The excess nitrogen (N) deposition by wet scavenging and dry removal processes could lead to loss of biodiversity [Bergström and Jansson, 2006; Simkin *et al.*, 2016], acidification [Rodhe *et al.*, 2002], enhanced emissions of N_2O from coastal waters [Seitzinger and Kroese, 1998] and carbon accumulation in the atmosphere under future climate change [Zaehle *et al.*, 2010]. The acidic sulfur (S) deposition can threaten the quality of soil and water as well [Driscoll *et al.*, 2001; McDonnell *et al.*, 2013]. Though large reduction of sulfur dioxide (SO_2) and nitrogen oxides ($\text{NO}_x = \text{NO} + \text{NO}_2$) emissions has been achieved over United States during the past 20 years [Smith *et al.*, 2011; Vet *et al.*, 2014], the threat of excess N, S, and N + S depositions still exists [Burns *et al.*, 2011; Nanus *et al.*, 2012; Sullivan *et al.*, 2012; Lovett, 2013]. The emission of ammonia (NH_3) in United States has increased by 11% from 1990 to 2010 [Xing *et al.*, 2013] and their combined effects remain critical stress to the environment at several regions. Critical load (CL) is commonly used to quantify the exceedance (i.e., Deposition > CL) of N, S, and N + S depositions. CL is defined as the criterion with the maximum one or more pollutants deposition above which significant harmful effects on specified sensitive elements of the environment are expected to accrue [Nilsson and Grennfelt, 1988; Gregor *et al.*, 2004].

© 2017 The Authors.

This is an open access article under the terms of the Creative Commons Attribution-NonCommercial-NoDerivs License, which permits use and distribution in any medium, provided the original work is properly cited, the use is non-commercial and no modifications or adaptations are made.

To assess current and future exceedances, the global climate-chemistry models are usually good alternatives to provide long-term trends of N, S, and N + S depositions. Since individual models are sensitive to specific configurations such as initial and boundary conditions, resolution and atmospheric chemical reactions, the multimodel mean (MMM) usually outperforms any single model [Reichler and Kim, 2008] and is commonly used to improve the model performance given the variability and uncertainty among models. Lamarque *et al.* [2005] used six different tropospheric chemistry models to calculate the N deposition pertaining to 2000 and 2100 conditions under the Intergovernmental Panel on Climate Change (IPCC) Special Report on Emissions Scenarios (SRES) A2 scenario. The MMM provided a good estimation of wet NO_3^- deposition in United States compared to measurements from National Atmospheric Deposition Program (NADP). The wet NO_3^- deposition was projected to increase strongly in the future due to the globally enhanced N emission. The split between dry and wet deposition rates was very model dependent and the ratio of dry deposition over wet deposition was projected to increase slightly in the future. However, the missing of NH_3 emission in that study could lead to significant underestimation of N deposition. Dentener *et al.* [2006] used 23 atmospheric chemistry transport models from the Atmospheric Composition Change: the European NeTwork of excellence (ACCENT) IPCC Fourth Assessment Report (AR4) modeling exercise to calculate the present (2000) and future (2030) global deposition of N_r and SO_x . About 74%, 65%, and 66% of the modeled NO_y , NH_x , and SO_x depositions were within 50% of the measurements from United States in 2000. The projected deposition in 2030 suggested that the benefit of reduction in NO_y deposition could be offset by the increased NH_x deposition, which meant that the latter metric would be a key factor in the future. However, one disadvantage of that work was that an empirical value ($10 \text{ kg [N] ha}^{-1} \text{ yr}^{-1}$) was used for CL exceedance analysis, which was just the lower threshold value for sensitive ecosystem. Sanderson *et al.* [2008] used 15 chemistry-transport models from Task Force on Hemispheric Transport of Air Pollution (TF HTAP) to quantify the NO_y deposition over four regions (Europe, North America, South Asia, and East Asia). The model evaluation showed that 69% of modeled results agreed within $\pm 50\%$ of the observations. Nevertheless, only one year (2001) simulation was conducted and the influence of interannual variability on the deposition could not be assessed. Lamarque *et al.* [2013b] had evaluated the historical and projected N and S depositions from the Atmospheric Chemistry and Climate Model Intercomparison Project (ACCMIP). The MMM showed good agreement between the modeled and observed wet NO_3^- , NH_4^+ , and SO_4^{2-} depositions in United States, with around 70% of simulation data falling within $\pm 50\%$ of the observations. The projected NO_y and SO_x depositions under representative concentration pathways scenarios [RCPs, van Vuuren *et al.*, 2011 and references therein] decreased dramatically while the projected NH_x deposition clearly increased in United States, which was also indicated from their earlier work [Lamarque *et al.*, 2011]. However, the dry deposition from MMM was not explored in Lamarque *et al.* [2013b]. Zhang *et al.* [2012] used the global chemical transport model (GEOS-Chem) with $0.5^\circ \times 0.67^\circ$ nested horizontal resolution to analyze the distribution, sources, and processes of N deposition over the North America. Ellis *et al.* [2013] adopted the same framework to further investigate the present and future N deposition to national parks, using the CL synthesized by Pardo *et al.* [2011]. It seemed that most present-day (2006) CL exceedance of N deposition to U.S. national parks was anthropogenic in origin and mainly dominated by NO_y . However, opposite to the projected large decrease of NO_x emissions under RCPs in 2050, the projected stronger NH_3 emission was likely to cause higher NH_x deposition. Nevertheless, only one year simulation to represent the present year in 2006 and the future year in 2050 was conducted in Ellis *et al.* [2013] and the same meteorology and natural emissions from 2006 were used for the 2050 simulation, thus neglecting the impact from weather and climate change.

According to the previous studies, MMM is likely to provide more reliable estimate of N and S depositions in United States. A few studies used MMM to investigate the CL exceedance of N deposition on the ecosystem but a uniform CL of $10 \text{ kg (N) ha}^{-1} \text{ yr}^{-1}$ is assumed, which fails to consider the spatial heterogeneity of acid deposition resistance over various land use types. Recent study has showed that using a uniform value could sometimes misinterpret the sensitivity of ecosystem to acid depositions from the perspective of either gross plant community or individual species [Lovett, 2013; Simkin *et al.*, 2016]. Therefore, in this study, we use the CL from the work of McNulty *et al.* [2013], where the N, S, and N + S depositions are separately used to calculate the corresponding CL values based on the steady-state mass balance equations (SMBEs). Further description is provided in Section 2.3 and more details about the calculation of CL can be found in McNulty *et al.* [2007, 2013]. The MMM from ACCMIP is used to unfold the N ($\text{NO}_y + \text{NH}_x$), S ($\text{SO}_2 + \text{SO}_4^{2-}$), and N + S depositions to the forest soil over the conterminous U.S. (CONUS) for the present and future years. Note

that the CL exceedance caused by the N, S, and N + S depositions is estimated by the sum of wet and dry deposition throughout the rest of study.

2. Methodology

2.1. Ensemble Simulations of Deposition

The ACCMIP provides an insight into the evolution of atmospheric chemistry under historical and future climate change [Lamarque *et al.*, 2013a]. It consists of a series of numerical time slice experiments to explore atmospheric chemistry driven by the climatic changes from the Coupled Model Intercomparison Project Phase 5 [CMIP5, Taylor *et al.*, 2012] simulations. The anthropogenic and biomass burning emissions are based on Lamarque *et al.* [2010] for the present-day simulation and the projected emissions for short-lived precursors follow the RCPs. The ACCMIP data are archived at the British Atmospheric Data Centre (<http://badc.nerc.ac.uk>) and detailed descriptions about participating models, simulation configuration, and evaluation of present-day climate are well documented by Lamarque *et al.* [2013a]. The provided monthly model outputs (NH_3 , NH_4^+ , $\text{NO}_y = \text{NO} + \text{NO}_2 + \text{HNO}_3 + \text{HNO}_4 + \text{NO}_3^- + \text{N}_2\text{O}_5 + \text{PAN}$ + other organic nitrates [Sun *et al.*, 2016], SO_2 , and SO_4^{2-}) are linearly interpolated from the native horizontal resolutions to the $0.1^\circ \times 0.1^\circ$ grid resolution (finer than any single model, about 8 km over the CONUS) in order to match the resolution of CL data that will be described below. As indicated by Lamarque *et al.* [2013a], several models generate the necessary data for the historical NO_y deposition, but fewer models have NH_x and S depositions. In this study, the MMM for specific species is calculated using all the available model results. The 2000 time slice (4–10 years simulation among models) is used to represent the present years (2000s), while 2050 (5–10 years simulation among models) time slice under RCP 8.5 scenario [Riahi *et al.*, 2007] is used for the future years (2050s). The availability of species from different global climate-chemistry models and time slices is shown in Table S1, Supporting Information.

2.2. Dry Deposition Data From Clean Air Status and Trends Network

For the wet N and S depositions, the evaluation conducted by Lamarque *et al.* [2013b] had showed that MMM was in good agreement with NADP observation as mentioned above. Thus model performance of simulated wet deposition is not presented in this study. However, the dry N and S depositions have not been evaluated yet. Different from the wet deposition which is calculated by concentrations of species and precipitation volumes both from measurements [Walker *et al.*, 2012b], the dry deposition is derived from the measured air concentrations at the Clean Air Status and Trends Network (CASTNET) sites and the simulated dry deposition velocity from the multilayer model (MLM) [Saylor *et al.*, 2014]. The calculation of dry deposition velocity takes the following form:

$$V_d = \left[R_a + \left(\int_0^{h_c} S(z) dz + \frac{1}{r_{\text{soil}} + r_{a,\text{soil}}} \right)^{-1} \right]^{-1} \quad (1)$$

where V_d is the deposition velocity (unit: m s^{-1}); R_a is the aerodynamic resistance (unit: s m^{-1}); h_c is the height of the canopy (unit: m); $S(z)$ is the general local sink term for trace species deposition to the canopy (unit: s^{-1}); r_{soil} is the soil uptake resistance (unit: s m^{-1}) and $r_{a,\text{soil}}$ is the subcanopy aerodynamic resistance for deposition to soil (unit: s m^{-1}). The dry deposition data is archived by U.S. EPA (<http://www.epa.gov/castnet/>) and about 90 sites that cover the entire or partial periods of 2000–2009 are used in this study for model comparison in 2000s.

2.3. Critical Load

As mentioned above, CL is by definition a threshold below which negative impacts do not occur. The value and impact of CL depend not only on the receptors [Pardo *et al.*, 2011], but also on the specific type of adverse effect [Bouwman *et al.*, 2002; Baron, 2006]. The CL used in this study is from the work of McNulty *et al.* [2013], which focuses on the soil acidification in the forested system that covers 68.6% areas of CONUS. Unlike the previous studies only focusing on the N deposition in United States [Lamarque *et al.*, 2005; Dentener *et al.*, 2006; Ellis *et al.*, 2013], the S deposition is still supposed to cause soil acidification and must be considered as well. The CL is calculated by using the SMBEs with N and S inputs, sinks, and outputs. The SMBEs approach has taken the water and soil chemistry, mineral soil weathering rates, deposition level and the ecosystem responses to chemical changes (i.e., uptake rate of base cations and N for 28 forest

type groups generated from United States Department of Agriculture, https://data.fs.usda.gov/geodata/rastergateway/forest_type/) into account, more representative than the empirical approach. A critical load function is first formed in order to estimate the CL and this function is defined by three thresholds: minimum critical load value for N ($CL_{\min}(N)$), maximum critical load value for N ($CL_{\max}(N)$), and maximum critical load value for S ($CL_{\max}(S)$). These three thresholds can be calculated by the following equations (http://www.rivm.nl/media/documenten/cce/manual/mapman_5_3.pdf):

$$CL_{\min}(N) = N_i + N_u \quad (2)$$

$$CL_{\max}(S) = BC_{\text{dep}} - Cl_{\text{dep}} - Bc_u + CL(A) \quad (3)$$

$$CL_{\max}(N) = CL_{\min}(N) + \frac{CL_{\max}(S)}{1 - f_{de}} \quad (4)$$

where N_i is the long-term net immobilization of N in soil organic matter; N_u is the net removal of N in harvested vegetation and animals; BC_{dep} is the total deposition of base cations (i.e., Na + Ca + Mg + K); Cl_{dep} is the chloride deposition; Bc_u is the uptake flux of base cations except Na (i.e., Ca + Mg + K) due to forest harvesting; $CL(A)$ is the critical load of acidity and f_{de} is denitrification fraction. The $CL_{\min}(N)$, $CL_{\max}(S)$, and $CL_{\max}(N)$ should be interpreted as: (1) If N deposition is lower than $CL_{\min}(N)$, only S deposition matters for the exceedance assessment; (2) If the N deposition is higher than $CL_{\max}(N)$, N deposition alone can adversely harm the forest soil; (3) If the N deposition is between $CL_{\min}(N)$ and $CL_{\max}(N)$, N deposition alone is less likely to cause negative impact; (4) N + S deposition is always examined for the CL exceedance with the CL in this case defined as $CL_{\min}(N) + CL_{\max}(S)$ (summed $CL_{\min}(N)$ and $CL_{\max}(S)$ values, since they are converted to the same unit). Note that $CL_{\min}(N)$, $CL_{\max}(S)$, and $CL_{\max}(N)$ vary spatially and are computed by (3) and (4) with the assumption of zero denitrification fraction over the CONUS, which means $CL_{\max}(N)$ equals to $CL_{\min}(N) + CL_{\max}(S)$. Note that in the SMBEs, the uptake of S by vegetation is generally insignificant. Thus, unlike for N deposition, there is only one CL value for S deposition and it is termed as $CL_{\max}(S)$. The CL with the resolution 12 km × 12 km can be downloaded from the NADP website (<http://nadp.isws.illinois.edu/committees/clad/db/>). It is further regressed to the regular 0.1° × 0.1° grid to keep its regional representation of surface type and can be matched by the resolution of ACCMIP MMM (Figure S1).

3. Results and Discussion

3.1. Model Comparison for Dry HNO_3 , NH_4^+ , SO_2 , and SO_4^{2-} Depositions

The 10-year (2000–2009, may not cover the whole period for different models based on their availability) averaged annual dry deposition from CASTNET sites, MMM, and each model output are represented as box plots for HNO_3 , NH_4^+ , SO_2 , and SO_4^{2-} , respectively (Figures 1a–1d). It seems that different individual models can vary dramatically from each other, especially for HNO_3 . Clear underestimation [e.g., MOCAGE and HadGEM2; *Josse et al.*, 2004; *Collins et al.*, 2011] and overestimation [e.g., CMAM and NCAR_CAM3.5; *Scinocca et al.*, 2008; *Lamarque et al.*, 2012] of HNO_3 dry deposition are observed, which could be attributed to the differences of their total NO_x emissions (table S2.3 in *Lamarque et al.* [2013a]) and the treatment of soil NO_x emission (table 3 in *Lamarque et al.* [2013a]). Models like UM_CAM [*Zeng et al.*, 2008] also show large variance, which should be related to their relatively coarse resolutions (Table S1). Based on the scatter plots for MMM (Figures 1e–1h), the slope is close to 1.0 except for NH_4^+ and the correlation coefficients are all higher than 0.75 except for HNO_3 . About 66% and 77% of modeled HNO_3 and SO_4^{2-} data are within ±50% of the CASTNET values, while the percentages for NH_4^+ and SO_2 are only 38% and 18%, respectively. For NH_4^+ , the emission of NH_3 has large discrepancies among the regions in United States [*Heald et al.*, 2012; *Walker et al.*, 2012a], which can significantly contribute to the bias here. The higher estimation of SO_2 dry deposition may be caused by the overestimated surface SO_2 concentration due to the uncertainty of emission rates and deficiency in the dry removal scheme among global chemistry-climate models [*Roelofs et al.*, 1998; *Knote et al.*, 2011; *Buchard et al.*, 2014]. The intercepts of the scatter plots reveal that there are systematic positive differences for MMM, especially at the sites with low dry deposition. Previous literature suggests that dry deposition is more difficult to estimate due to the surface types [*Hidy et al.*, 2011]. It is strongly influenced by the atmospheric chemistry, meteorology, terrain complexity, and biological characteristics [*Lovett, 1994*;

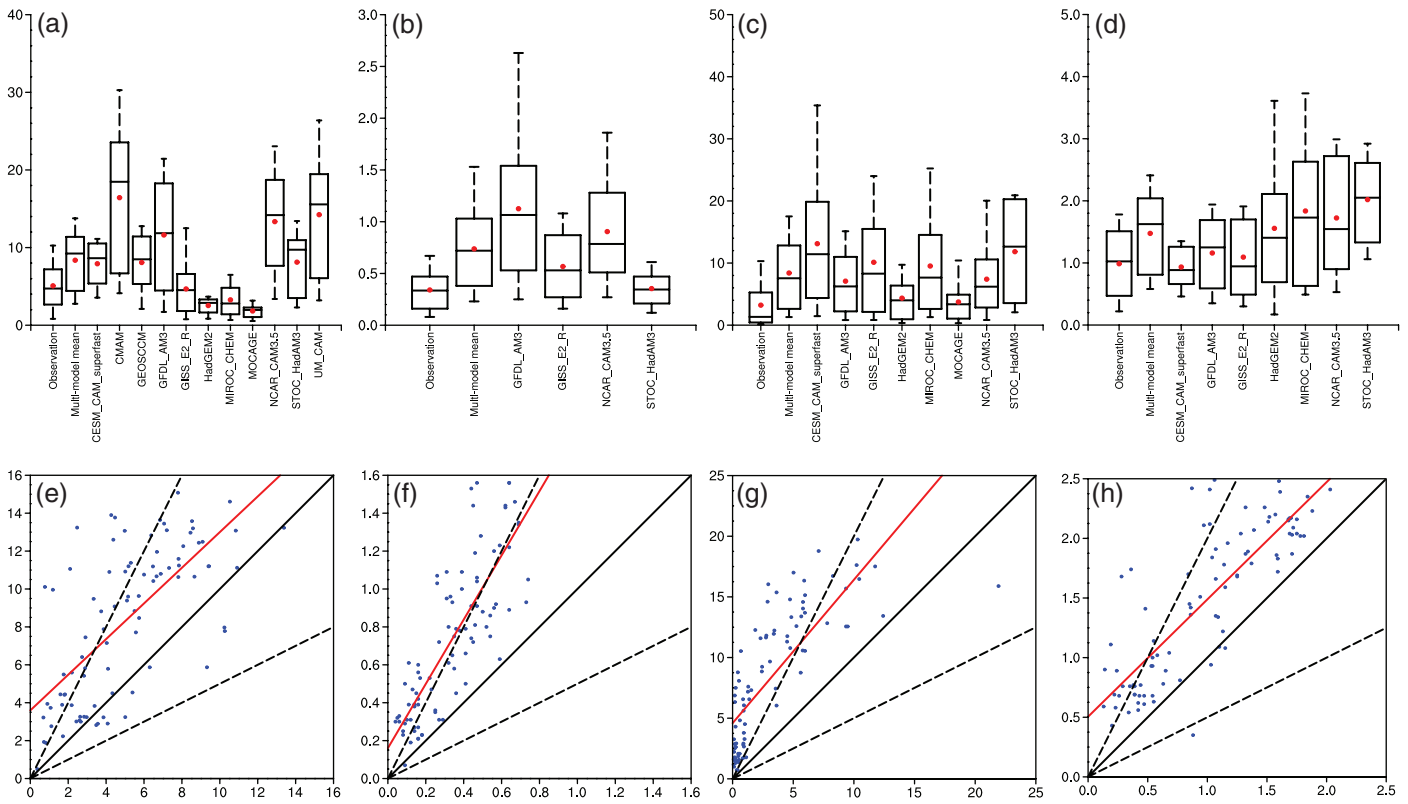


Figure 1. Box plots of 10-year (2000–2009, may not cover the whole period for different models) averaged annual total dry deposition from CASTNET sites, multimodel mean (MMM) and each model output for (a) HNO₃, (b) NH₄⁺, (c) SO₂, and (d) SO₄²⁻, respectively. The top and bottom horizontal lines for each box correspond to the 95th and 5th percentiles. The second, third, and fourth horizontal lines of the box from top to bottom are the 75th, 50th, and 25th percentiles of the data range. The red dot in each box represents the mean value. The scatter plots are MMM result (y-axis) versus observation (x-axis) for (e) HNO₃, (f) NH₄⁺, (g) SO₂, and (h) SO₄²⁻, respectively. Dashed lines indicate \pm factor 1:2 and 2:1 and the red solid line is the result of least-square linear regression.

Clarke et al., 1997]. Finkelstein et al. [2000] found that the dry deposition velocity for SO₂ at forested canopies was underestimated by 35%, and Schwede et al. [2011] pointed out that the estimated dry deposition velocity at CASTNET sites for SO₂ and HNO₃ was likely to be 50% and 35% lower, respectively. Clarke et al. [1997] estimated that the uncertainty of CASTNET observation for SO₂ and HNO₃ is 30% and 40% or larger, respectively. Fowler et al. [2009] suggested that the uncertainty of dry deposition fluxes for main chemical species (e.g., HNO₃) was about 50% and similar percent was reported for SO₂ by Nowlan et al. [2014]. The uncertainty could be even larger due to the irregular terrain or forested canopies over Eastern U.S. [Sickles and Shadwick, 2015]. On the other hand, the coarse resolution of global climate-chemistry models might not describe the vegetation well, which caused uncertainty of simulating the surface-atmosphere interactions [Verbeke et al., 2015]. Other factors such as simplified chemistry and limited representation of physics and transport could also worsen the model performance [Hauglustaine et al., 2014]. The statistics for MMM and each model output indicate that for HNO₃, either positive or negative differences from CASTNET can be observed among models while for the other three species, consistent positive differences are found (Table S2). For individual model like GFDL_AM3 [Naik et al., 2013], it only predicts the dry deposition well for SO₄²⁻. Other models (e.g., GISS_E2_R [Shindell et al., 2013]) may perform well for some species (e.g., HNO₃, NH₄⁺, and SO₄²⁻) but its paired comparison of statistic parameters (e.g., MNB and MNE) varies largely, which suggests that both positive and negative differences exist inside the model among the CASTNET sites. Instead, the MMM for each species considers the uncertainties of individual models and provides consistent results for a given pair of statistic parameters. It is also relatively close to the CASTNET data based on the box plots (Figures 1a–1d). Therefore, it is more appropriate to use MMM to calculate the CL exceedance due to N, S, and N + S depositions.

3.2. Exceedance of N, S, and N + S Depositions in 2000s and 2050s

Based on the definition by *Karl and Koss* [1984], we divide the CONUS into nine climate regions (Northeast, Southeast, South, Central, East North Central, West North Central, Southwest, West and Northwest, Figure S2). The spatial distribution of N, S, and N + S depositions from MMM over the CONUS shows that the strongest deposition appears in the regions like Central (e.g., Ohio and Indiana) and Northeast (e.g., Pennsylvania) in 2000s (Figures S3a, S3c and S3e). Totally 99.07% of the forest soil over the CONUS is estimated to have N deposition higher than the $CL_{min}(N)$, which means that the N deposition is not negligible for the exceedance analysis over most part of the CONUS. In addition, N deposition over 10.32% of the forest soil over the CONUS in 2000s exceeds the corresponding $CL_{max}(N)$, suggesting that N deposition alone may cause environmental concern there. The percentages of $CL_{max}(N)$ exceeded areas from each climate region over the national total $CL_{max}(N)$ exceeded areas show that Northeast (47.34%) and East North Central (26.18%) have the highest N deposition (Table 1a), including Michigan and Pennsylvania where the N emission from power plant and industry is strong. Other states like Indiana and Wisconsin may have less forest soil affected, but the exceedance amount there could be still high ($\sim 500 \text{ eq ha}^{-1} \text{ yr}^{-1}$, Figure 2a). For the 0.93% of the forest soil over the CONUS where the N deposition is lower than the $CL_{min}(N)$, about 500 km² areas receive the S deposition that is higher than the $CL_{max}(S)$. All the $CL_{max}(S)$ exceeded areas are in West (Figure 2c), which indicates that the S deposition alone could still threaten the environment even though the N deposition is not a concern there.

On the other hand, the N + S deposition over 30.16% of the forest soil over the CONUS exceed the $CL_{min}(N) + CL_{max}(S)$ in 2000s (Figure 2e) and it mainly affects the Eastern U.S. with the largest percent in Central (32.89%), followed by Northeast (24.74%) and East North Central (20.84%) (Table 1a). Many more CL exceeded areas are observed in these three regions (e.g., Pennsylvania, Michigan, and Indiana), with the maximum exceedance amount even higher than 1000 eq ha⁻¹ yr⁻¹. It is worth noting that the forest soil in Central seems to be less impacted by the N deposition (Table 1a). However, the largest CL exceedance percent appears when the N + S deposition is considered, due to the strong sulfur emission from power plant and industry there. The impact of S deposition to the ecosystem is usually missed by the previous N deposition studies [*Lamarque et al.*, 2005; *Dentener et al.*, 2006; *Sanderson et al.*, 2008; *Lamarque et al.*, 2013b] and thus highlighted in this work. The results here are generally consistent with those in the study of *McNulty et al.* [2013] and both studies emphasize that the S deposition cannot be ignored for soil acidification. Nevertheless, our estimated national exceedance percent of N + S deposition is relatively higher than that estimated by *McNulty et al.* [2013] (around 22%). Potential reasons for this difference include the positive bias from MMM results (Section 3.1), different temporal scale for deposition (1994–2000 in *McNulty et al.* [2013] but 2000–2009 in this study) and the limited species from CASTNET observations (only NO₃⁻ and NH₄⁺ for wet deposition and particulate NH₄⁺ and HNO₃ for dry deposition). The ratio of N deposition over S deposition is further calculated for the forest soil over the CONUS where the N + S deposition exceeds the corresponding $CL_{min}(N) + CL_{max}(S)$. When the exceedance amount is less than 400 eq ha⁻¹ yr⁻¹, the ratio is usually much higher than 1 (~ 3 in East North Central, Figure S4a and 2e), which means that N deposition dominates the effect. However, when the exceedance amount is more than 1000 eq ha⁻¹ yr⁻¹ (e.g., Central and Northeast), the ratio rapidly drops with value close to 1, indicating that the S deposition is playing an important role over there and necessary to be included for the exceedance analysis. It is also observed that N deposition has already caused vital environmental concern in Central (e.g., Indiana), East North Central (e.g., Michigan), Northeast (e.g., New Jersey), and Southeast (e.g., Florida). The high exceedance percentages from N + S deposition in East North Central, Central, and Northeast suggest that continued ecological impacts to forests. Therefore, policy- and decision-makers should pay specific attention to those regions.

The total N, S, and N + S depositions are projected to decrease nationwide by 2050 (Figure S3b, S3d and S3f). The N, S, and N + S depositions to the forest soil over the CONUS from 2000s to 2050s are likely to decrease by about 28.7%, 81.4%, and 50.5%, respectively. This is due to the strongly reduced emissions of sulfur and NO_x over the CONUS under the RCP 8.5 scenario [*Riahi et al.*, 2007]. The N deposition to the 97.75% of the forest soil over the CONUS is higher than the $CL_{min}(N)$ and thus still important for the exceedance assessment despite decreased NO_x emissions. Based on Table 1a, the $CL_{max}(N)$ exceeded areas caused by N deposition in 2050s are much smaller than that in 2000s. Except Southwest and Northwest, all the other seven climate regions are projected to have fewer $CL_{max}(N)$ exceeded areas with the largest absolute difference at

Table 1. Summary of the Critical Load (CL) Exceeded Forest Soil Over the CONUS (Unit: km², Rounded to the Nearest 1000) and the Percent of CL Exceeded Areas for Each Climate Region in 2000s and 2050s, Respectively

	Climate Regions									
						West East				
	West		Southwest		South	Southeast		Northwest	Central	
	(%)	(%)	(%)	(%)	(%)	(%)	(%)	(%)	(%)	(%)
(a) Use the CL aggregated from the average values of 12 × 12 grids from 1-km resolution										
National CL _{max} (N) exceeded areas in 2000s: 551,000 km ²										
P_N_2000s	0.02	0.21	0.77	10.88	0.00	1.39	26.18	13.21	47.34	
National CL _{max} (N) exceeded areas in 2050s: 81,000 km ²										
P_N_2050s	0.00	1.41	3.53	11.08	0.00	5.59	62.03	11.26	5.08	
National CL _{max} (S) exceeded areas in 2000s: 500 km ²										
P_S_2000s	100.00	0.00	0.00	0.00	0.00	0.00	0.00	0.00	0.00	0.00
National CL _{max} (S) exceeded areas in 2050s: 0 km ²										
P_S_2000s	0.00	0.00	0.00	0.00	0.00	0.00	0.00	0.00	0.00	0.00
National CL _{min} (N) + CL _{max} (S) exceeded areas in 2000s: 1,611,000 km ²										
P_N_S_2000s	1.54	0.19	2.89	15.85	0.06	1.00	20.84	32.89	24.74	
National CL _{min} (N) + CL _{max} (S) exceeded areas in 2050s: 160,000 km ²										
P_N_S_2050s	0.00	0.72	1.98	14.84	0.00	4.44	57.51	12.91	7.60	
(b) Use the CL aggregated from the minimum values of 12 × 12 grids from 1-km resolution										
National CL _{max} (N) exceeded areas in 2000s: 1,304,000 km ²										
P_N_2000s	0.08	0.17	3.66	20.53	0.00	1.84	25.95	17.13	30.64	
National CL _{max} (N) exceeded areas in 2050s: 567,000 km ²										
P_N_2050s	0.03	0.31	2.01	20.57	0.00	3.89	46.57	6.09	20.53	
National CL _{max} (S) exceeded areas in 2000s: 1000 km ²										
P_S_2000s	100.00	0.00	0.00	0.00	0.00	0.00	0.00	0.00	0.00	0.00
National CL _{max} (S) exceeded areas in 2050s: 0 km ²										
P_S_2050s	0.00	0.00	0.00	0.00	0.00	0.00	0.00	0.00	0.00	0.00
National CL _{min} (N) + CL _{max} (S) exceeded areas in 2000s: 2,634,000 km ²										
P_N_S_2000s	2.35	0.59	13.96	23.04	1.00	1.16	17.14	23.95	16.81	
National CL _{min} (N) + CL _{max} (S) exceeded areas in 2050s: 759,000 km ²										
P_N_S_2050s	0.05	0.28	2.96	20.59	0.02	3.18	39.16	12.63	21.12	
(c) Use the CL aggregated from the maximum values of 12 × 12 grids from 1-km resolution										
National CL _{max} (N) exceeded areas in 2000s: 111,000 km ²										
P_N_2000s	0.09	0.61	1.78	8.26	0.00	2.22	16.83	20.02	50.18	
National CL _{max} (N) exceeded areas in 2050s: 17,000 km ²										
P_N_2050s	0.00	3.92	8.54	15.92	0.00	11.22	24.92	30.66	4.82	
National CL _{max} (S) exceeded areas in 2000s: 400 km ²										
P_S_2000s	100.00	0.00	0.00	0.00	0.00	0.00	0.00	0.00	0.00	0.00
National CL _{max} (S) exceeded areas in 2050s: 0 km ²										
P_S_2050s	0.00	0.00	0.00	0.00	0.00	0.00	0.00	0.00	0.00	0.00
National CL _{min} (N) + CL _{max} (S) exceeded areas in 2000s: 925,000 km ²										
P_N_S_2000s	1.41	0.26	1.10	7.46	0.04	0.58	15.74	41.72	31.69	
National CL _{min} (N) + CL _{max} (S) exceeded areas in 2050s: 25,000 km ²										
P_N_S_2050s	0.00	2.68	9.24	20.86	0.00	10.85	23.86	27.73	4.77	

Table 1. (continued)

	(d) The same as (a) but using CL with the consideration of climate change								
	National $CL_{max}(N)$ exceeded areas in 2050s: 51,000 km ²								
P_N_2050s	0.00	2.23	5.18	11.12	0.00	7.57	54.64	14.51	4.74
	National $CL_{max}(S)$ exceeded areas in 2050s: 0 km ²								
P_S_2050s	0.00	0.00	0.00	0.00	0.00	0.00	0.00	0.00	0.00
	National $CL_{max}(N) + CL_{max}(S)$ exceeded areas in 2000s: 100,000 km ²								
P_N_S_2050s	0.00	1.15	2.87	18.66	0.00	5.02	56.48	10.35	5.46

P_N_2000s, The percent of $CL_{max}(N)$ exceeded areas for each climate region in 2000s.; P_N_2050s, The percent of $CL_{max}(N)$ exceeded areas for each climate region in 2050s.; P_S_2000s, The percent of $CL_{max}(S)$ exceeded areas for each climate region in 2000s.; P_S_2050s, The percent of $CL_{max}(S)$ exceeded areas for each climate region in 2050s.; P_N_S_2000s, The percent of $CL_{min}(N) + CL_{max}(S)$ exceeded areas for each climate region in 2000s.; P_N_S_2050s, The percent of $CL_{min}(N) + CL_{max}(S)$ exceeded areas for each climate region in 2050s.

Northeast (~257,000 km²). The N deposition over 1.52% of national forest soil exceeds the $CL_{max}(N)$ and the exceedance amount is mostly lower than 400 eq ha⁻¹ yr⁻¹ (Figure 2b). East North Central (62.03%) is likely to experience most exceedance of N deposition (e.g., Michigan and Indiana) while Northeast yields the highest $CL_{max}(N)$ exceedance percent in 2000s. For the 2.25% of the forest soil over the CONUS where the N deposition is lower than the $CL_{min}(N)$, the S deposition is all lower than the $CL_{max}(S)$ (Figure 2d). The $CL_{max}(S)$ exceedance in West in 2000s diminishes in 2050s, which suggests that S deposition alone is less likely to cause an environmental concern in 2050s. Moreover, all nine climate regions are projected to have fewer $CL_{min}(N) + CL_{max}(S)$ exceeded areas with the largest absolute difference in Central (~509,000 km²). In 2050s, 2.99% of the forest soil over the CONUS is projected to have N + S deposition exceeding the corresponding $CL_{min}(N) + CL_{max}(S)$ and the exceedance amount is mostly lower than 500 eq ha⁻¹ yr⁻¹ as well (Figure 2f). Both the $CL_{min}(N) + CL_{max}(S)$ exceeded areas and exceedance amount are much smaller than those in 2000s (Figure 2e). The highest percent of exceedance is 57.51% in East North Central, while the Central dominates in 2000s. The ratio of N deposition over S deposition is generally higher than 4 for the forest soil where the $CL_{min}(N) + CL_{max}(S)$ is exceeded and could be even higher than 7 at the East North Central (Figure S4b), indicating that N deposition is likely to be more crucial when considering the exceedance of N + S deposition in 2050s.

3.3. Contributions of NO_y and NH_x Depositions to N Deposition

We further explore the contributions of NO_y and NH_x depositions to the N deposition in 2000s and 2050s, respectively. The NH_x deposition has been assumed to be readily converted to N compounds such as nitrate that can acidify. The ratio of NO_y deposition over NH_x deposition is generally higher than 1 for most forest soil over the CONUS in 2000s and could be even higher than 5 for the west and east coast, illustrating that NO_y deposition dominates the N deposition in 2000s (Figure S5a). The NO_y and NH_x depositions to 91.93% and 63.62% of the forest soil over the CONUS exceed the $CL_{min}(N)$, respectively. The national total percentages of $CL_{max}(N)$ exceeded areas caused by NO_y and NH_x depositions are 3.32% and 0.06% in 2000s, respectively (Figures 3a and 3c). In the regional perspective, Northeast (62.25%) has the highest $CL_{max}(N)$ exceeded percent caused by NO_y deposition while Central (55.06%) has the highest $CL_{max}(N)$ exceeded percent caused by NH_x deposition (Table 2). Higher exceedance amount caused by NO_y deposition (>300 eq ha⁻¹ yr⁻¹, Figure 3a) could be observed at states such as New Jersey and Indiana. For Florida, the NO_y deposition can also lead to exceedance of $CL_{max}(N)$ probably due to the relatively low $CL_{max}(N)$ values (Figure S1) and strong NO_x emission from vehicles (<https://www.epa.gov/air-emissions-inventories>).

In 2050s, the ratio of NO_y deposition over NH_x deposition in coastal region is nationwide smaller than 3 (Figure S5b), which is much lower than that in 2000s. Moreover, the ratio in the regions such as Central and East North Central is even smaller than 1. This suggests that the NH_x deposition could play a relatively more important role in the future, due to the reduced NO_y emission but enhanced NH₃ emission under RCP 8.5 projection [Riahi *et al.*, 2007]. The NO_y and NH_x depositions to 84.07% and 71.72% of the forest soil over the CONUS are projected to exceed the $CL_{min}(N)$ in 2050s, respectively. All the nine climate regions are consistently projected to have fewer $CL_{max}(N)$ exceeded areas caused by NO_y deposition (Table 2), with the largest absolute difference in Northeast (~110,000 km²). However, NH_x deposition is found to cause more

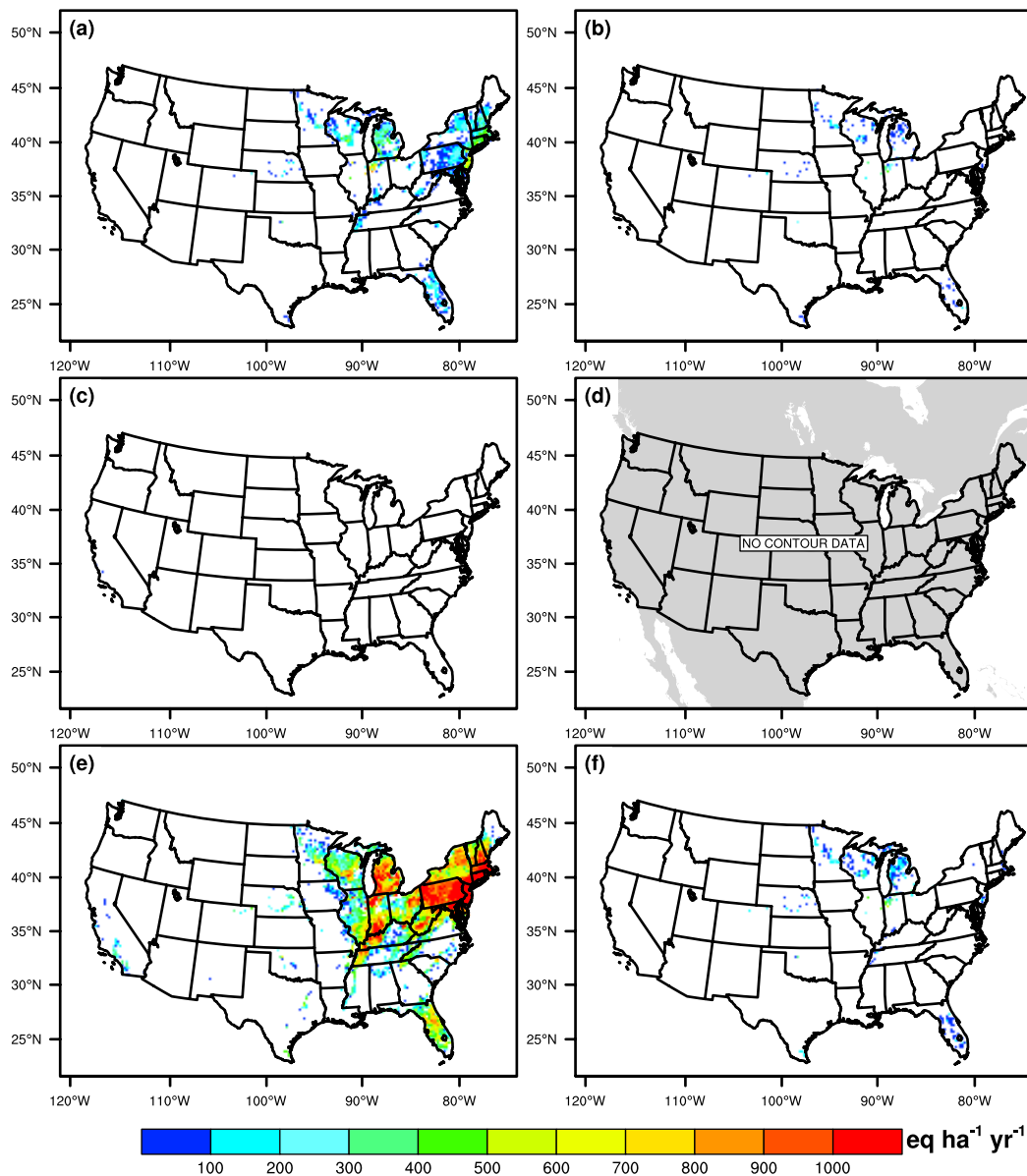


Figure 2. The critical load (CL) exceedance amount (unit: $\text{eq ha}^{-1} \text{yr}^{-1}$) in 2000s based on the (a) $\text{CL}_{\max}(\text{N})$, (b) $\text{CL}_{\max}(\text{S})$, and (c) $\text{CL}_{\min}(\text{N}) + \text{CL}_{\max}(\text{S})$, respectively, (b), (d), and (f) are the same but for 2050s.

$\text{CL}_{\max}(\text{N})$ exceeded areas with the largest absolute difference in East North Central ($\sim 1000 \text{ km}^2$). The percent of national total $\text{CL}_{\max}(\text{N})$ exceeded areas caused by NO_y deposition (0.02%) is also lower than that caused by NH_x deposition (0.1%) in 2050s (Figures 3b and 3d). This highlights the more important role of NH_x deposition in the future exceedance analysis since further reduction of NO_y emission will only help alleviate the $\text{CL}_{\max}(\text{N})$ exceedance caused by the N deposition, not the NH_x deposition. Note that East North Central yields high percent of $\text{CL}_{\max}(\text{N})$ exceedance caused by either NO_y or NH_x deposition in 2050s. Considering the fact that the $\text{CL}_{\max}(\text{N})$ exceeded areas caused by N deposition are also larger in East North Central than any other regions (Table 1a), this may be the most critical region that deserves the special attention for the $\text{CL}_{\max}(\text{N})$ exceedance analysis of future N deposition.

3.4. Upper and Lower Bounds of Exceedance by N, S, and N + S Depositions

In the work of McNulty et al. [2013], the CL dataset is originally calculated at 1-km resolution. However, NADP and NCLD (National Critical Load Database) further aggregate it into the resolution of $12 \text{ km} \times 12 \text{ km}$ for

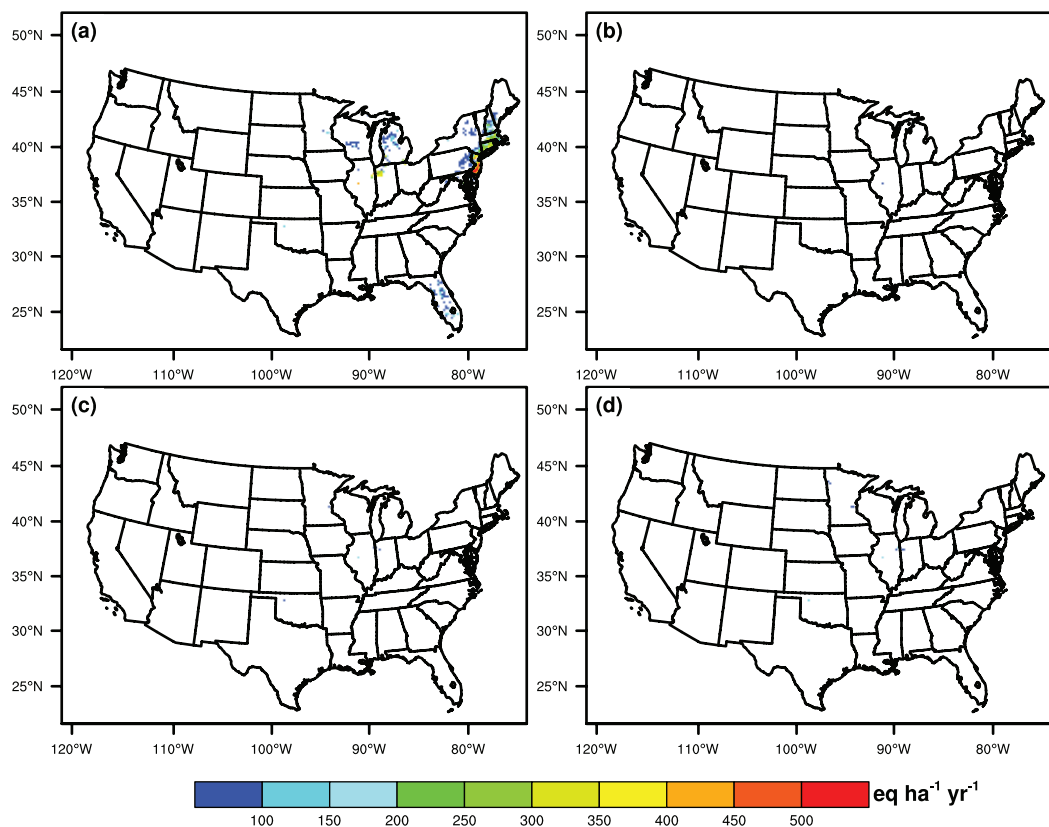


Figure 3. $CL_{\max}(N)$ exceedance caused by (a) NO_x deposition and (c) NH_x deposition for the forest soil over the CONUS in 2000s (unit: $eq\ ha^{-1}\ yr^{-1}$), (b) and (d) are the same but for 2050s.

public download. In the analysis above, the CL data aggregated by averaging the values of $12\ km \times 12\ km$ grids from 1-km resolution is used. There are also another two aggregation metrics, which take the minimum and maximum values of $12\ km \times 12\ km$ grids from 1-km resolution, respectively. Hence, we can use these two metrics to identify the upper and lower bounds of the CL exceedance over the CONUS.

Using the minimum CL values (Figure S6), N deposition to 99.71% of the forest soil over the CONUS is higher than the $CL_{\min}(N)$, which is almost the same as that in Section 3.2. However, the national $CL_{\max}(N)$ exceeded percent is 24.42% while the $CL_{\min}(N) + CL_{\max}(S)$ exceeded percent is 49.32% in 2000s (Figures 4a and 4e). These two percentages are much higher than those in Section 3.2 (10.32% [Figure 2a] and 30.16% [Figure 2e]) and the $CL_{\max}(N)$ and $CL_{\min}(N) + CL_{\max}(S)$ exceeded percentages are likely to increase largely in regions such as East North Central, Central and Southeast (Table 1b). This indicates that for those regions, lots of forest soil is under the marginal threat of N and N + S depositions. Therefore, using a lower CL will increase the CL exceeded percent significantly. It is also worth noting that for regions like East North Central and Northeast, using the minimum $CL_{\min}(N) + CL_{\max}(S)$ values would lead to more areas with exceedance amount higher than $1000\ eq\ ha^{-1}\ yr^{-1}$. For the rest 0.29% of the forest soil over the CONUS whose N deposition is lower than $CL_{\min}(N)$, about $1000\ km^2$ areas receive the S deposition higher than the corresponding $CL_{\max}(S)$ (Figure 4c), which is twice higher than that in Section 3.2 ($\sim 500\ km^2$).

In 2050s, the N deposition to 98.82% of the forest soil over the CONUS is higher than the $CL_{\min}(N)$. 10.61% and 14.21% of the forest soil will be adversely affected by the N and N + S depositions, respectively (Figures 4b and 4f). Though many regions show lower percentages than those in Section 3.2, the absolute CL exceeded areas are still higher since the national total CL exceeded areas are higher (Tables 1a and 1b). Note that the CL exceeded percentages in regions like Northeast have increased significantly, suggesting that much forest soil in those regions may still be under the marginal threat of N and N + S depositions in 2050s even though the NO_x and SO_2 are projected to decrease. For the rest 1.18% of the forest soil where the N deposition is lower than $CL_{\min}(N)$, the S deposition alone is still lower than the corresponding $CL_{\max}(S)$.

Table 2. Summary of $CL_{max}(N)$ Exceeded Forested Areas Over the CONUS (Unit: km^2 , Rounded to the Nearest 1000) and the $CL_{max}(N)$ Exceeded Percent for Each Climate Region Caused by NO_y or NH_x Deposition Alone in 2000s and 2050s, Respectively

	Climate Regions									
	West					East				
	West (%)	Southwest (%)	South (%)	Southeast (%)	Northwest (%)	North (%)	Central (%)	Central (%)	Central (%)	Northeast (%)
NO_y deposition										
National $CL_{max}(N)$ exceeded areas in 2000s: $177,000 km^2$										
P_N_2000s	0.00	0.11	0.51	13.68	0.00	0.26	17.57	5.63	62.25	
National $CL_{max}(N)$ exceeded areas in 2050s: $1000 km^2$										
P_N_2050s	0.00	0.00	0.00	0.00	0.00	0.00	38.19	38.85	22.96	
NH_x deposition										
National $CL_{max}(N)$ exceeded areas in 2000s: $3,000 km^2$										
P_N_2000s	0.00	0.00	9.28	0.00	0.00	0.00	35.66	55.06	0.00	
National $CL_{max}(N)$ exceeded areas in 2050s: $5,000 km^2$										
P_N_2050s	0.00	0.00	10.92	0.00	0.00	6.68	39.82	42.59	0.00	

(Figure 4d), similar to that in Section 3.2. Overall, the minimum CL values contribute to the highest $CL_{max}(N)$ and $CL_{min}(N) + CL_{max}(S)$ exceedance for the forest soil over the CONUS, which could be treated as the upper bound for the deposition exceedance assessment.

On the other hand, by using the maximum CL values (Figure S7), N deposition to 95.65% of the forest soil over the CONUS is higher than the $CL_{min}(N)$ in 2000s, whose percent is lower than that in Figure S6 since the $CL_{min}(N)$ is higher here. However, only 2.09% and 17.32% of the forest soil is under the threat of N and N + S depositions, respectively (Figures 5a and 5e). For the rest 4.35% of the forest soil whose N deposition is lower than $CL_{min}(N)$, about $400 km^2$ areas exceed their corresponding $CL_{max}(S)$ by S deposition, which is also lower than the results above (Figure 5c). The $CL_{max}(N)$ and $CL_{min}(N) + CL_{max}(S)$ exceeded percent for the forest soil over the CONUS will be further reduced to 0.32% and 0.47% in 2050s, respectively (Figures 5b and 5f). The S deposition alone is all lower than the $CL_{max}(S)$ as before (Figure 5d). It is worth noting that the CL exceeded percentages in Northeast and Central are even higher than those in Section 3.2 (Tables 1a and 1c), mainly due to their high CL exceedance amount (Figure 2). Nevertheless, more $CL_{max}(N)$ and $CL_{min}(N) + CL_{max}(S)$ exceeded areas are also observed in West North Central and Southeast in 2050s, which is mainly due to their relatively high CL exceedance amount but low maximum CL values. In a word, fewest areas of the forest soil over the CONUS are adversely affected by the N, S, and N + S depositions with the maximum CL values and the assessment results here can be treated as the lower bound of CL exceedance.

3.5. Impact of Climate Change on the Exceedance by N, S, and N + S Depositions

In the previous sections, we estimate the CL exceedance based on the CL developed at the present level. It is reported in the IPCC Fifth Assessment Report [Collins *et al.*, 2013] that the global mean surface temperature is projected to increase by approximately $2^\circ C$ through 2050s. The enhanced temperature could increase the base cation weathering, the cation uptake, and the runoff term of the SMBEs. McNulty *et al.* [2013] found out that a $4^\circ C$ increase in the air temperature could contribute to a 20% increase in the base cation weathering. Since base cation weathering rate is thought as the most critical parameter in the sensitivity analysis of the SMBEs [Li and McNulty, 2007], we further explore the impact of the change of temperature from 2000s to 2050s on the CL values and its associated CL exceedance over the CONUS. The monthly mean air temperature from models in ACCMIP is used to generate the annual mean air temperature different between 2050s and 2000s (2050s – 2000s). Then we apply the relationship reported by McNulty *et al.* [2013] ($4^\circ C$ increase in the air temperature versus 20% increase in the base cation weathering) to update the base cation weathering in (3) (part of the CL(A) term). Finally the N, S, and N + S depositions in 2050s is used to reevaluate the CL exceedance with the updated CL values including the consideration of climate change (Figure S8). The

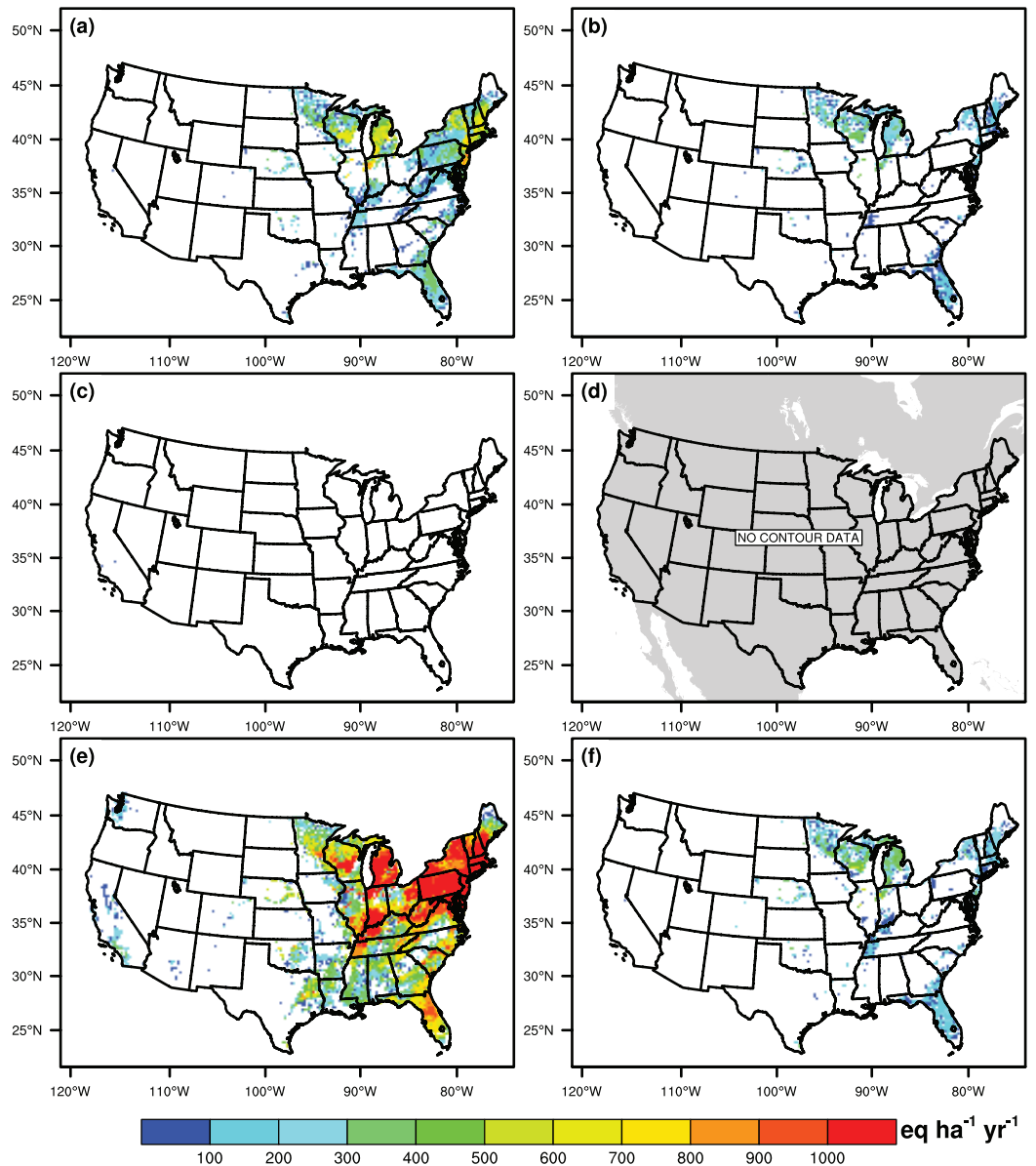


Figure 4. CL exceedance amount (unit: $\text{eq ha}^{-1} \text{yr}^{-1}$) for the forest soil over the CONUS in 2000s based on the (a) $\text{CL}_{\max}(\text{N})$, (c) $\text{CL}_{\max}(\text{S})$, and (e) $\text{CL}_{\min}(\text{N}) + \text{CL}_{\max}(\text{S})$ aggregated by using the minimum values of $12 \text{ km} \times 12 \text{ km}$ grids at 1-km resolution, (b), (d), and (f) are the same but for 2050s.

$\text{CL}_{\min}(\text{N})$ is not affected by the base cation weathering rate and thus the CL exceeded areas with the update $\text{CL}_{\min}(\text{N})$ are the same as those in Section 3.2. Thus it turns out that N deposition to 97.75% of the forest soil over the CONUS again exceeds the updated $\text{CL}_{\min}(\text{N})$. Clear reduction of CL exceeded areas caused by the N and N + S depositions is found over the CONUS (Figures 6a and 6c). When Table 1d and Table 1a compared, the national total CL exceeded areas caused by N deposition have decreased by approximately $30,000 \text{ km}^2$ with the updated $\text{CL}_{\max}(\text{N})$. Six climate regions show fewer $\text{CL}_{\max}(\text{N})$ exceeded areas with the largest reduction in East North Central ($\sim 22,000 \text{ km}^2$). For the rest 2.25% of the forest soil over the CONUS where the N deposition is lower than the updated $\text{CL}_{\min}(\text{N})$, the S deposition alone is less likely to cause CL exceedance anywhere based on the updated CL. The N + S deposition to about $100,000 \text{ km}^2$ of the forest soil over the CONUS could exceed the updated $\text{CL}_{\min}(\text{N}) + \text{CL}_{\max}(\text{S})$, whose areas are around $60,000 \text{ km}^2$ fewer than those shown in Table 1a. The maximum reduction of $\text{CL}_{\min}(\text{N}) + \text{CL}_{\max}(\text{S})$ exceeded areas is in East North Central ($\sim 36,000 \text{ km}^2$), followed by Central ($\sim 10,000 \text{ km}^2$). Recalling the (3), the increased base cation weathering

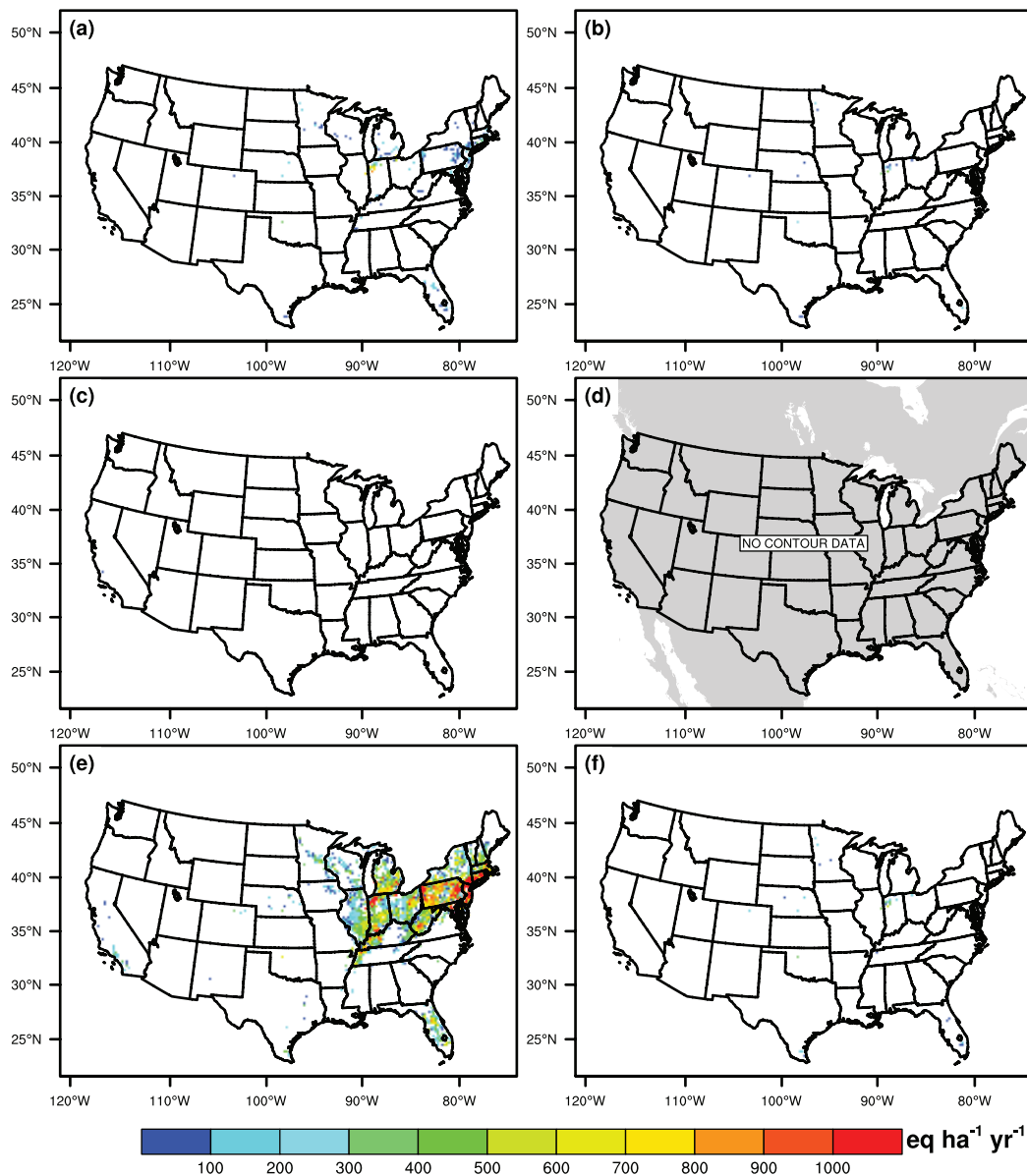


Figure 5. CL exceedance amount (unit: $\text{eq ha}^{-1} \text{yr}^{-1}$) for the forest soil over the CONUS in 2000s based on the (a) $\text{CL}_{\text{max}}(\text{N})$, (c) $\text{CL}_{\text{max}}(\text{S})$, and (e) $\text{CL}_{\text{min}}(\text{N}) + \text{CL}_{\text{max}}(\text{S})$ aggregated by using the maximum values of $12 \text{ km} \times 12 \text{ km}$ grids at 1-km resolution, (b), (d), and (f) are the same but for 2050s.

rate due to the rising air temperature will increase the CL(A), which consequently increases the $\text{CL}_{\text{max}}(\text{S})$ and $\text{CL}_{\text{max}}(\text{N})$. Therefore, since S deposition alone is not able to cause CL exceedance in 2050s with the original $\text{CL}_{\text{max}}(\text{S})$ (see Section 3.2), it is obvious that S deposition alone will not cause any CL exceedance with the updated $\text{CL}_{\text{max}}(\text{S})$ (Figure 6b). It also makes sense that CL exceeded areas caused by the N + S deposition with the updated $\text{CL}_{\text{min}}(\text{N}) + \text{CL}_{\text{max}}(\text{S})$ will be fewer.

4. Conclusion

To our knowledge, this work is the first to analyze the exceedance of N + S deposition to the forest soil over the CONUS using output from multiple global climate-chemistry models in 2000s and 2050s. The exceedance is assessed by the CL that considers both N and S depositions and the variety of surface types. We also first projected the future CL with respect to the increased air temperature under climate change. The MMM from ACCMIP output shows a good agreement with observation for the wet NO_3^- , NH_4^+ , and

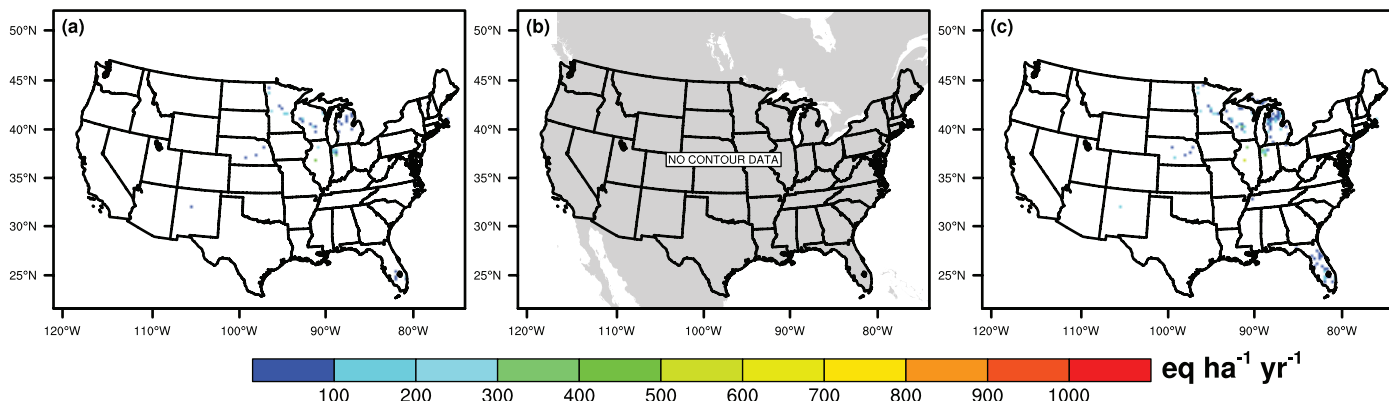


Figure 6. CL exceedance amount (unit: $\text{eq ha}^{-1} \text{yr}^{-1}$) for the forest soil over the CONUS in 2050s based on the updated (a) $\text{CL}_{\text{max}}(\text{N})$, (b) $\text{CL}_{\text{max}}(\text{S})$, and (c) $\text{CL}_{\text{min}}(\text{N}) + \text{CL}_{\text{max}}(\text{S})$ with the consideration of increased temperature under climate change.

SO_4^{2-} depositions in the previous work [Lamarque *et al.*, 2013b] and the dry deposition comparison in this study also indicates that MMM can represent the dry HNO_3 , NH_3 , and SO_4^{2-} depositions well, except certain overestimate for the dry SO_2 deposition at low amount. Compared to the CL aggregated by averaging the 12 km × 12 km grids from 1-km resolution, all the forest soil over the CONUS receives N deposition higher than $\text{CL}_{\text{min}}(\text{N})$, meaning that N deposition could not be neglected for the exceedance analysis. In 2000s, 10.32% of the forest soil over the CONUS experiences N deposition higher than their corresponding $\text{CL}_{\text{max}}(\text{N})$ and the highest $\text{CL}_{\text{max}}(\text{N})$ exceeded percent is in Northeast. For regions like Central, the $\text{CL}_{\text{max}}(\text{N})$ exceeded percent may not be high but the exceedance amount can be larger than 500 $\text{eq ha}^{-1} \text{yr}^{-1}$. Totally 30.16% of the forest soil over the CONUS is classified as $\text{CL}_{\text{min}}(\text{N}) + \text{CL}_{\text{max}}(\text{S})$ exceeded areas and the largest $\text{CL}_{\text{min}}(\text{N}) + \text{CL}_{\text{max}}(\text{S})$ exceeded percent is in Central. It reveals that around three times more forest soil over the CONUS will exceed the CL by considering the N + S deposition, which highlights the importance of involving S deposition in this study. The ratio of N deposition over S deposition in 2000s also suggests the critical contribution of S deposition when it decreases to 1.5 or less. Under the RCP 8.5 scenario, due to the strong reduction of projected NO_x and sulfur emissions, there are fewer $\text{CL}_{\text{max}}(\text{N})$ and $\text{CL}_{\text{min}}(\text{N}) + \text{CL}_{\text{max}}(\text{S})$ exceeded areas in 2050s and the exceedance amount is mostly lower than 400 $\text{eq ha}^{-1} \text{yr}^{-1}$.

In addition, with respect to N deposition alone, the ratio of NO_y deposition over NH_x deposition is generally higher than 1 for most forest soil over the CONUS in 2000s, indicating that the NO_y deposition is more crucial. The national $\text{CL}_{\text{max}}(\text{N})$ exceeded percentages caused by NO_y and NH_x depositions are about 3.32% and 0.06%, respectively. The ratio drops to smaller than 1 over several regions in 2050s and more forest soil over the CONUS is adversely affected by the NH_x deposition, implying the relatively more importance of NH_x deposition. The projected high $\text{CL}_{\text{max}}(\text{N})$ exceeded percentages generally locate at the middle CONUS, where agriculture is a strong source of NH_3 emission. Regulating NH_3 emission is therefore necessary considering the control purpose. It is also worth noting although the individual NO_y or NH_x deposition leads to much fewer $\text{CL}_{\text{max}}(\text{N})$ exceeded areas than the summed N deposition, it could still harm the forest soil considerably in the regions like East North Central.

The upper and lower bounds of deposition exceedance for the forest soil over the CONUS are also assessed by using the minimum and maximum CL values of 12 km × 12 km grids from 1-km resolution, respectively. Applying the minimum values of CL will lead to 11.71, 2.74, and 2.85 times $\text{CL}_{\text{max}}(\text{N})$, $\text{CL}_{\text{max}}(\text{S})$, and $\text{CL}_{\text{min}}(\text{N}) + \text{CL}_{\text{max}}(\text{S})$ exceed areas than applying the maximum values of CL in 2000s. By using the minimum values of CL instead of the maximum ones, 32.69 and 29.93 times $\text{CL}_{\text{max}}(\text{N})$ and $\text{CL}_{\text{min}}(\text{N}) + \text{CL}_{\text{max}}(\text{S})$ exceed areas are projected in 2050s. It indicates that the forest soil in many regions over the CONUS are under the marginal threat of N, S, and N + S depositions and the results of CL exceedance can vary significantly from different selections of CL, especially in 2050s. The impact of climate change on the analysis of CL exceedance is further examined. Due to the projected nationwide increase of temperature in the future, the values of $\text{CL}_{\text{max}}(\text{S})$ and $\text{CL}_{\text{max}}(\text{N})$ will consequently grow and thus contribute to even fewer $\text{CL}_{\text{max}}(\text{N})$ and $\text{CL}_{\text{min}}(\text{N}) + \text{CL}_{\text{max}}(\text{S})$ exceeded areas. We think the results from this study, considering the influence of

Acknowledgments

The authors acknowledge the Critical Loads of Atmospheric Deposition (CLAD) Science Committee of the NADP for their role in making available CLAD_CL_ACID_v2.accdb and CLAD_CL_N_v2.accdb datasets. This paper has not been subjected to EPA peer and administrative review; therefore, the conclusions and opinions contained herein are solely those of the authors, and should not be construed to reflect the views of the EPA. The output data from the Atmospheric Chemistry and Climate Model Intercomparison Project (ACCMIP) are archived at the British Atmospheric Data Centre (<http://badc.nerc.ac.uk>) and the 12-km resolution of CL data for the forest soil over the CONUS is archived at (<http://nadp.sws.uiuc.edu/committees/clad/db/>).

aggregation methods and climate change, can be used as a reference of exceedance range for the assessment of N, S, and N + S depositions to the policy- and decision-makers.

References

- Baron, J. S. (2006), Hindcasting nitrogen deposition to determine an ecological critical load, *Ecol. Appl.*, 16(2), 433–439. [https://doi.org/10.1890/1051-0761\(2006\)016\[0433:HNDTDA\]2.0.CO;2](https://doi.org/10.1890/1051-0761(2006)016[0433:HNDTDA]2.0.CO;2).
- Bergström, A.-K., and M. Jansson (2006), Atmospheric nitrogen deposition has caused nitrogen enrichment and eutrophication of lakes in the Northern Hemisphere, *Global Change Biol.*, 12(4), 635–643. <https://doi.org/10.1111/j.1365-2486.2006.01129.x>.
- Bouwman, A. F., D. P. Van Vuuren, R. G. Derwent, and M. Posch (2002), A global analysis of acidification and eutrophication of terrestrial ecosystems, *Water Air Soil Pollut.*, 141, 349–382. <https://doi.org/10.1023/A:1021398008726>.
- Buchard, V., A. M. da Silva, P. Colarco, N. Krotkov, R. R. Dickerson, J. W. Stehr, G. Mount, E. Spinei, H. L. Arkinson, and H. He (2014), Evaluation of GEOS-5 sulfur dioxide simulations during the Frostburg, MD 2010 field campaign, *Atmos. Chem. Phys.*, 14(4), 1929–1941. <https://doi.org/10.5194/acp-14-1929-2014>.
- Burns, D. A., J. A. Lynch, B. J. Cosby, M. E. Fenn, and J. S. Baron (2011), National Acid Precipitation Assessment Program Report to Congress 2011: An integrated assessment, US EPA Clean Air Markets Div., Natl. Sci. and Technol. Counc., Washington, D. C., 114 pp.
- Clarke, J. F., E. S. Edgerton, and B. E. Martin (1997), Dry deposition calculations for the clean air status and trends network, *Atmos. Environ.*, 31(21), 3667–3678. [https://doi.org/10.1016/S1352-2310\(97\)00141-6](https://doi.org/10.1016/S1352-2310(97)00141-6).
- Collins, M., et al. (2013), Long-term climate change: Projections, commitments and irreversibility, in *Climate Change 2013: The Physical Science Basis. Contribution of Working Group I to the Fifth Assessment Report of the Intergovernmental Panel on Climate Change*, edited by T. F. Stocker, D. Qin, G.-K. Plattner, M. Tignor, S. K. Allen, J. Boschung, A. Nauels, Y. Xia, V. Bex, and P. M. Midgley, Cambridge Univ. Press, Cambridge, U. K.
- Collins, W. J., et al. (2011), Development and evaluation of an Earth-System model – HadGEM2, *Geosci. Model Dev.*, 4, 1051–1075. <https://doi.org/10.5194/gmd-4-1051-2011>.
- Dentener, F., et al. (2006), Nitrogen and sulfur deposition on regional and global scales: A multimodel evaluation, *Global Biogeochem. Cycle.*, 20, GB4003. <https://doi.org/10.1029/2005GB002672>.
- Driscoll, C. T., G. B. Lawrence, A. J. Bulger, T. J. Butler, C. S. Cronan, C. Eagar, K. F. Lambert, G. E. Likens, J. L. Stoddard, and K. C. Weathers (2001), Acidic deposition in the northeastern United States: sources and inputs, ecosystem effects, and management strategies, *BioScience*, 51(3), 180–198. [https://doi.org/10.1641/0006-3568\(2001\)051\[0180:ADITNU\]2.0.CO;2](https://doi.org/10.1641/0006-3568(2001)051[0180:ADITNU]2.0.CO;2).
- Ellis, R. A., D. J. Jacob, M. P. Sulprizio, L. Zhang, C. D. Holmes, B. A. Schichtel, T. Blett, E. Porter, L. H. Pardo, and J. A. Lynch (2013), Present and future nitrogen deposition to national parks in the United States: critical load exceedances, *Atmos. Chem. Phys.*, 13, 9083–9095. <https://doi.org/10.5194/acp-13-9083-2013>.
- Finkelstein, P. L., T. G. Ellestad, J. F. Clarke, T. P. Meyers, D. B. Schwede, E. O. Hebert, and J. A. Neal (2000), Ozone and sulfur dioxide dry deposition to forests: Observations and model evaluation, *J. Geophys. Res.*, 105(D12), 15,365–15,377. <https://doi.org/10.1029/2000JD900185>.
- Fowler, D., et al. (2009), Atmospheric composition change: Ecosystems–Atmosphere interactions, *Atmos. Environ.*, 43(33), 5193–5267. <https://doi.org/10.1016/j.atmosenv.2009.07.068>.
- Galloway, J. N., et al. (2004), Nitrogen cycles: Past, present, and future, *Biogeochemistry*, 70(2), 153–226. <https://doi.org/10.1007/s10533-004-0370-0>.
- Gregor, H. D., B. Werner, and T. Spranger (2004), *Manual on Methodologies and Criteria for Mapping Critical Levels/Loads and Geographical Areas where They Are Exceeded*, ICP Modeling and Mapping, Berlin, Germany, 212 pp.
- Hauglustaine, D. A., Y. Balkanski, and M. Schulz (2014), A global model simulation of present and future nitrate aerosols and their direct radiative forcing of climate, *Atmos. Chem. Phys.*, 14, 11031–11063. <https://doi.org/10.5194/acp-14-11031-2014>.
- Heald, C. L., et al. (2012), Atmospheric ammonia and particulate inorganic nitrogen over the United States, *Atmos. Chem. Phys.*, 12, 10,295–10,312. <https://doi.org/10.5194/acp-12-10295-2012>.
- Hidy, G. M., J. R. Brook, K. L. Demerjian, L. T. Molina, W. T. Pennell, and R. D. Scheffe (2011), *Technical Challenges of Multipollutant Air Quality Management*, Springer, New York, 172 pp.
- Josse, B., P. Simon, and V. H. Peuch (2004), Radon global simulations with the multiscale chemistry and transport model MOCAGE, *Tellus Ser. B*, 56(4), 339–356. <https://doi.org/10.1111/j.1600-0889.2004.00112.x>.
- Karl, T. R., and W. J. Koss (1984), *Regional and National Monthly, Seasonal, and Annual Temperature Weighted by Area, 1895–1983*, Historical Climatology Series 4-3, National Climatic Data Center, Asheville, N. C., 38 pp.
- Knote, C., et al. (2011), Towards an online-coupled chemistry-climate model: Evaluation of trace gases and aerosols in COSMO-ART, *Geosci. Model Dev.*, 4(4), 1077–1102. <https://doi.org/10.5194/gmd-4-1077-2011>.
- Lamarque, J.-F., et al. (2005), Assessing future nitrogen deposition and carbon cycle feedback using a multimodel approach: Analysis of nitrogen deposition, *J. Geophys. Res.*, 110, D19303. <https://doi.org/10.1029/2005JD005825>.
- Lamarque, J.-F., et al. (2010), Historical (1850–2000) gridded anthropogenic and biomass burning emissions of reactive gases and aerosols: Methodology and application, *Atmos. Chem. Phys.*, 10(15), 7017–7039. <https://doi.org/10.5194/acp-10-7017-2010>.
- Lamarque, J.-F., G. P. Kyle, M. Meinshausen, K. Riahi, S. J. Smith, D. P. van Vuuren, A. Conley, and F. Vitt (2011), Global and regional evolution of short-lived radiatively-active gases and aerosols in the Representative Concentration Pathways, *Clim. Change*, 109, 191–212. <https://doi.org/10.1007/s10584-011-0155-0>.
- Lamarque, J.-F., et al. (2012), CAM-chem: Description and evaluation of interactive atmospheric chemistry in the Community Earth System Model, *Geosci. Model Dev.*, 5(2), 369–411. <https://doi.org/10.5194/gmd-5-369-2012>.
- Lamarque, J.-F., et al. (2013a), The Atmospheric Chemistry and Climate Model Intercomparison Project (ACCMIP): Overview and description of models, simulations and climate diagnostics, *Geosci. Model Dev.*, 6(1), 179–206. <https://doi.org/10.5194/gmd-6-179-2013>.
- Lamarque, J.-F., et al. (2013b), Multi-model mean nitrogen and sulfur deposition from the Atmospheric Chemistry and Climate Model Intercomparison Project (ACCMIP): Evaluation of historical and projected future changes, *Atmos. Chem. Phys.*, 13(16), 7997–8018. <https://doi.org/10.5194/acp-13-7997-2013>.
- Li, H., and S. G. McNulty (2007), Uncertainty analysis on simple mass balance model to calculate critical loads for soil acidity, *Environ. Pollut.*, 149(3), 315–326. <https://doi.org/10.1016/j.envpol.2007.05.014>.
- Lovett, G. M. (1994), Atmospheric deposition of nutrients and pollutants in North America: An ecological perspective, *Ecol. Appl.*, 4(4), 629–650. <https://doi.org/10.2307/1941997>.

- Lovett, G. M. (2013), Critical issues for critical loads, *Proc. Natl. Acad. Sci. U. S. A.*, **110**(3), 808–809. <https://doi.org/10.1073/pnas.1219007110>.
- McDonnell, T. C., T. J. Sullivan, B. J. Cosby, W. A. Jackson, and K. J. Elliott (2013), Effects of climate, land management, and sulfur deposition on soil base cation supply in national forests of the southern appalachian mountains, *Water Air Soil Pollut.*, **224**, 1733–1750. <https://doi.org/10.1007/s11270-013-1733-8>.
- McNulty, S. G., E. C. Cohen, J. A. M. Myers, T. J. Sullivan, and H. Li (2007), Estimates of critical acid loads and exceedances for forest soils across the conterminous United States, *Environ. Pollut.*, **149**, 281–292. <https://doi.org/10.1016/j.envpol.2007.05.025>.
- McNulty, S. G., E. C. Cohen, and J. A. Moore Myers (2013), Climate change impacts on forest soil critical acid loads and exceedances at a national scale, in *Forest Health Monitoring: National Status, Trends, and Analysis 2010, Gen. Tech. Rep. SRS-GTR-176*, edited by K. M. Potter, B. L. Conkling, pp. 95–108, U.S. Department of Agriculture Forest Service, Southern Research Station, Asheville, N. C.
- Naik, V., L. W. Horowitz, A. M. Fiore, P. Ginoux, J. Mao, A. M. Aghedo, and H. Levy II (2013), Impact of preindustrial to present-day changes in short-lived pollutant emissions on atmospheric composition and climate forcing, *J. Geophys. Res. Atmos.*, **118**, 8086–8110. <https://doi.org/10.1002/jgrd.50608>.
- Nanus, L., D. W. Clow, J. E. Saros, V. C. Stephens, and D. H. Campbell (2012), Mapping critical loads of nitrogen deposition for aquatic ecosystems in the rocky mountains, USA, *Environ. Pollut.*, **166**, 125–135. <https://doi.org/10.1016/j.envpol.2012.03.019>.
- Nilsson, J. and P. Grennfelt (1988), Critical load for sulphur and nitrogen, report from a workshop at Skolster, Sweden, *NORD Rep. 9179960960 and 8773032484*, 418 pp, Nordic Counc. of Ministers, Copenhagen, Denmark.
- Nowlan, C. R., R. V. Martin, S. Philip, L. N. Lamsal, N. A. Krotkov, E. A. Marais, S. Wang, and Q. Zhang (2014), Global dry deposition of nitrogen dioxide and sulfur dioxide inferred from space-based measurements, *Global Biogeochem. Cycle.*, **28**(10), 1025–1043. <https://doi.org/10.1002/2014GB004805>.
- Olivier, J. G. J., A. F. Bouwman, C. W. M. van der Maas, J. J. M. Berdowski, C. Veldt, J. P. J. Bloos, A. J. H. Visschedijk, P. Y. J. Zandveld, and J. L. Haverlag (1996), Description of EDGAR version 2.0: A set of global emission inventories of greenhouse gases and ozone-depleting substances for all anthropogenic and most natural sources on a per country basis and on $1^\circ \times 1^\circ$ grid, *Natl. Inst. of Public Health and the Environ. (RIVM) Rep. 771060 002/TNO Rep. R96/119*. <http://www.rivm.nl/env/int/coredata/edgar>.
- Oman, L. D., J. R. Ziemke, A. R. Douglass, D. W. Waugh, C. Lang, J. M. Rodriguez, and J. E. Nielsen (2011), The response of tropical tropospheric ozone to ENSO, *Geophys. Res. Lett.*, **38**, L13706. <https://doi.org/10.1029/2011GL047865>.
- Pardo, L. H., et al. (2011), Effects of nitrogen deposition and empirical nitrogen critical loads for ecoregions of the United States, *Ecol. Appl.*, **21**(8), 3049–3082. <https://doi.org/10.1890/10-2341.1>.
- Reichler, T., and J. Kim (2008), How well do coupled models simulate today's climate? *Bull. Am. Meteorol. Soc.*, **89**(3), 303–311. <https://doi.org/10.1175/BAMS-89-3-303>.
- Riahi, K., A. Grübler, and N. Nakicenovic (2007), Scenarios of long-term socio-economic and environmental development under climate stabilization, *Technol. Forecast. Soc. Change*, **74**(7), 887–935. <https://doi.org/10.1016/j.techfore.2006.05.026>.
- Rodhe, H., F. Dentener, and M. Schulz (2002), The global distribution of acidifying wet deposition, *Environ. Sci. Technol.*, **36**(20), 4382–4388. <https://doi.org/10.1021/es020057g>.
- Roelofs, G.-J., J. Lelieveld, and L. Ganzeveld (1998), Simulation of global sulfate distribution and the influence on effective cloud drop radii with a coupled photochemistry sulfur cycle model, *Tellus Ser. B*, **50**(3), 224–242. <https://doi.org/10.1034/j.1600-0889.1998.t01-2-00002.x>.
- Sanderson, M. G., et al. (2008), A multi-model study of the hemispheric transport and deposition of oxidised nitrogen, *Geophys. Res. Lett.*, **35**, L17815. <https://doi.org/10.1029/2008GL035389>.
- Saylor, R. D., G. M. Wolfe, T. P. Meyers, and B. B. Hicks (2014), Technical note: A corrected formulation of the multilayer model (MLM) for inferring gaseous dry deposition to vegetated surfaces, *Atmos. Environ.*, **92**, 141–145. <https://doi.org/10.1016/j.atmosenv.2014.03.056>.
- Schweide, D., L. M. Zhang, R. Vet, and G. Lear (2011), An intercomparison of the deposition models used in the CASTNET and CAPMon networks, *Atmos. Environ.*, **45**(6), 1337–1346. <https://doi.org/10.1016/j.atmosenv.2010.11.050>.
- Scinocca, J. F., N. A. McFarlane, M. Lazare, J. Li, and D. Plummer (2008), Technical note: The CCCma third generation AGCM and its extension into the middle atmosphere, *Atmos. Chem. Phys.*, **8**, 7055–7074. <https://doi.org/10.5194/acp-8-7055-2008>.
- Seitzinger, S. P., and C. Kroeze (1998), Global distribution of nitrous oxide production and N inputs in freshwater and coastal marine ecosystems, *Global Biogeochem. Cycles*, **12**(1), 93–113. <https://doi.org/10.1029/97GB03657>.
- Shindell, D. T., et al. (2013), Interactive ozone and methane chemistry in GISS-E2 historical and future climate simulations, *Atmos. Chem. Phys.*, **13**, 2653–2689. <https://doi.org/10.5194/acp-13-2653-2013>.
- Sickles, J. E., II, and D. S. Shadwick (2015), Air quality and atmospheric deposition in the eastern US: 20 years of change, *Atmos. Chem. Phys.*, **15**, 173–197. <https://doi.org/10.5194/acp-15-173-2015>.
- Simkin, S. M., et al. (2016), Conditional vulnerability of plant diversity to atmospheric nitrogen deposition across the United States, *Proc. Natl. Acad. Sci. U. S. A.*, **113**(15), 4086–4091. <https://doi.org/10.1073/pnas.1515241113>.
- Smith, S. J., H. Pitcher, and T. M. L. Wigley (2001), Global and regional anthropogenic sulfur dioxide emissions, *Global Planet. Change*, **29**(1–2), 99–119. [https://doi.org/10.1016/S0921-8181\(00\)00057-6](https://doi.org/10.1016/S0921-8181(00)00057-6).
- Smith, S. J., J. van Aardenne, Z. Klimont, R. J. Andres, A. Volke, and S. Delgado Arias (2011), Anthropogenic sulfur dioxide emissions: 1850–2005, *Atmos. Chem. Phys.*, **11**, 1101–1116. <https://doi.org/10.5194/acp-11-1101-2011>.
- Stevenson, D. S., R. M. Doherty, M. G. Sanderson, W. J. Collins, C. E. Johnson, and R. G. Derwent (2004), Radiative forcing from aircraft NO_x emissions: mechanisms and seasonal dependence, *J. Geophys. Res.*, **109**, D17307. <https://doi.org/10.1029/2004JD004759>.
- Sullivan, T. J., B. J. Cosby, T. C. McDonnell, E. M. Porter, T. Blett, R. Haeuber, C. M. Huber, and J. A. Lynch (2012), Critical loads of acidity to protect and restore acid-sensitive streams in Virginia and West Virginia, *Water Air Soil Pollut.*, **223**, 5759–5771. <https://doi.org/10.1007/s11270-012-1312-4>.
- Sun, J., J. S. Fu, and H. Kan (2016), Organic nitrates and other oxidized nitrogen compounds contribute significantly to the total nitrogen depositions in the United States, *Proc. Natl. Acad. Sci. U. S. A.*, **113**(31), E4433–E4434. <https://doi.org/10.1073/pnas.1608717113>.
- Taylor, K. E., R. J. Stouffer, and G. A. Meehl (2012), An overview of CMIP5 and the experiment design, *Bull. Am. Meteorol. Soc.*, **93**(4), 485–498. <https://doi.org/10.1175/BAMS-D-11-00094.1>.
- van Vuuren, D. P., et al. (2011), The representative concentration pathways: An overview, *Clim. Change*, **109**, 5–31. <https://doi.org/10.1007/s10584-011-0148-z>.
- Verbeke, T., J. Lathiére, S. Szopa, and N. de Noblet-Ducoudré (2015), Impact of future land-cover changes on HNO₃ and O₃ surface dry deposition, *Atmos. Chem. Phys.*, **15**, 13,555–13,568. <https://doi.org/10.5194/acp-15-13555-2015>.
- Vet, R., et al. (2014), A global assessment of precipitation chemistry and deposition of sulfur, nitrogen, sea salt, base cations, organic acids, acidity and pH, and phosphorus, *Atmos. Environ.*, **93**, 3–100. <https://doi.org/10.1016/j.atmosenv.2013.10.060>.

- Vitousek, P. M., J. D. Aber, R. W. Howarth, G. E. Likens, P. A. Matson, D. W. Schindler, W. H. Schlesinger, and D. G. Tilman (1997), Human alteration of the global nitrogen cycle: Sources and consequences, *Ecol. Appl.*, 7(3), 737–750. [https://doi.org/10.1890/1051-0761\(1997\)007\[0737:HAOTGN\]2.0.CO;2](https://doi.org/10.1890/1051-0761(1997)007[0737:HAOTGN]2.0.CO;2).
- Walker, J. M., S. Philip, R. V. Martin, and J. H. Seinfeld (2012a), Simulation of nitrate, sulfate, and ammonium aerosols over the United States, *Atmos. Chem. Phys.*, 12, 11213–11227. <https://doi.org/10.5194/acp-12-11213-2012>.
- Walker, J. T., T. L. Dombek, L. A. Green, N. Gartman, and C. M. B. Lehmann (2012b), Stability of organic nitrogen in NADP wet deposition samples, *Atmos. Environ.*, 60, 573–582. <https://doi.org/10.1016/j.atmosenv.2012.06.059>.
- Watanabe, S., et al. (2011), MIROC-ESM 2010: Model description and basic results of CMIP5-20c3m experiments, *Geosci. Model Dev.*, 4, 845–872. <https://doi.org/10.5194/gmd-4-845-2011>.
- Xing, J., J. Pleim, R. Mathur, G. Pouliot, C. Hogrefe, C.-M. Gan, and C. Wei (2013), Historical gaseous and primary aerosol emissions in the United States from 1990 to 2010, *Atmos. Chem. Phys.*, 13, 7531–7549. <https://doi.org/10.5194/acp-13-7531-2013>.
- Zaehle, S., P. Friedlingstein, and A. D. Friend (2010), Terrestrial nitrogen feedbacks may accelerate future climate change, *Geophys. Res. Lett.*, 37, L01401. <https://doi.org/10.1029/2009GL041345>.
- Zeng, G., J. A. Pyle, and P. J. Young (2008), Impact of climate change on tropospheric ozone and its global budgets, *Atmos. Chem. Phys.*, 8, 369–387. <https://doi.org/10.5194/acp-8-369-2008>.
- Zhang, L., D. J. Jacob, E. M. Knipping, N. Kumar, J. W. Munger, C. C. Carouge, A. van Donkelaar, Y. X. Wang, and D. Chen (2012), Nitrogen deposition to the United States: Distribution, sources, and processes, *Atmos. Chem. Phys.*, 12, 4539–4554. <https://doi.org/10.5194/acp-12-4539-2012>.